
Article:
Li, NYD, Moore, DJ, Thompson, MA et al. (2 more authors) (2022) Influence of humectants on the thermotropic behaviour and nanostructure of fully hydrated lecithin bilayers. Chemistry and Physics of Lipids, 243. 105165. ISSN 0009-3084

https://doi.org/10.1016/j.chemphyslip.2021.105165

Influence of Humectants on the Thermotropic Behaviour and Nanostructure of Fully Hydrated Lecithin Bilayers

Ngai Ying Denise Li,[a,b,*] David J. Moore,[c] Michael A. Thompson,[d] Eloise Welfare[e] and Michael Rappolt[a,#]

[a] School of Food Science and Nutrition, University of Leeds, Leeds, LS2 9JT, U.K.
[b] School of Physics and Astronomy, University of Edinburgh, Edinburgh, EH9 3FD, U.K.
[c] Tioga Research, Edinburgh, U.K.
[d] GSK Consumer Healthcare, Skin Health R&D, Weybridge, U.K.
[e] GSK Business Service Centre, Quill 9, Jalan Semangat, 46300, Petaling Jaya, Malaysia.

Keywords: Humectants, DPPC, kosmotropes, SAXS, WAXS, differential scanning calorimetry.

Corresponding authors:
*Ngai Ying Denise Li: e-mail: denise.li@ed.ac.uk
#Michael Rappolt: e-mail: m.rappolt@leeds.ac.uk

Abstract

Humectants are used widely in topical formulations as they provide cosmetic and health benefits to skin. Of particular interest to our laboratories is the interaction of humectants in phospholipid based topical skin care formulations. This study probed the effects of three exemplary humectants on a fully hydrated lecithin system (DPPC) by use of X-ray scattering and differential scanning calorimetry. While the three humectants affected the nanostructure of 1, 2-dipalmitoyl-sn-glycero-3-phosphocholine, DPPC, bilayers in a similar manner; leading to an increased membrane order, differences in the effect on the thermal behaviour of DPPC suggest that betaine and sarcosine interacted via a different mechanism compared to acetic monoethanolamide, AMEA. At concentrations above 0.4 M, betaine and sarcosine stabilised the gel phase by depletion of the interfacial water via the preferential exclusion mechanism. At the same time, a slight increase in the rigidity of the membrane was observed with an increase in the membrane thickness. Overall, the addition of betaine or sarcosine resulted in an increase in the pre- and main transition temperatures of DPPC. AMEA, on the other hand, decreases both transition temperatures and although the interlamellar water layer was also decreased, there was evidence from the altered lipid chain packing, that AMEA molecules are present also at the bilayer interface, at least at high concentrations. Above the melting point in the fluid lamellar phase, none of the humectants induced significant structural changes, neither concerning the bilayer stacking order nor its overall membrane fluidity.

1. Introduction

Betaine, sarcosine and acetic monoethanolamide (AMEA), are water soluble humectants (Figure 1) and, as such, they are found in a wide range of applications in the food (Al-Muhtaseb et al., 2002; Syamaladevi et al., 2016) and cosmetic industries (Lodén, 2003). Specifically, humectants are used in many topical pharmaceutical and personal care products, including skin creams and haircare products (Gesslein, 1999). In dermatological formulations, humectants are delivered to the stratum corneum (SC), where, by helping to attract water, they support normal enzymatic activity and maintain SC plasticity. Betaine, sarcosine and AMEA are of particular interest to our laboratories as these humectants are used in several topical formulations under development. In addition to their hygroscopicity betaine, sarcosine, and AMEA are kosmotropes, therefore they favour remaining in the water phase and avoiding lipid/water interfacial regions when included in topical formulations or simple liposome systems (Söderlund et al., 2003). As a consequence, in fully hydrated lipid systems, kosmotropes stabilise the lamellar gel, L_β, and inverse hexagonal, H_{II}, phases (both, displaying relatively low water per lipid numbers (Rappolt et al., 2008)) over the fluid lamellar phase, L_α (Koynova et al., 1997; Tenchov et al., 1996).

In this study, we investigate the effect of three humectants on the thermotropic behaviour and nanostructure of fully hydrated 1, 2-dipalmitoyl-sn-glycero-3-phosphocholine (DPPC). Lecithins, such as DPPC, are used as functional ingredients in topical pharmaceutical and cosmetic formulations. However, DPPC and related lecithins have also been widely studied in the membrane biophysics community as models of the plasma membrane of cells. Consequently, the thermal behaviour and structural properties of DPPC have been extensively studied over the past several decades (Akutsu, 2020; Nagle et al., 1996; Pabst et al., 2004; Rappolt and Rapp, 1996; Wiener et al., 1989).

DPPC self-assembles into a lamellar structure in excess water, which is further distinguished into lamellar sub phases depending on temperature: the sub-gel, gel, ripple and fluid phase (Nagle and Tristram-Nagle, 2000; Rappolt et al., 2004). Since DPPC and other phospholipids are used in combination with humectants as structural and functional components in some topical dermatological formulations, it is valuable to understand their interactions. However, there is only limited published biophysical data characterising dermatological formulations, such as the structure of topical emulsions including de Vringer *et al.* (de Vringer et al., 1987) and more recently Ahmadi *et al.* (Ahmadi et al., 2021; Ahmadi et al., 2020). Of relevance to the current studies Rudolph and Goins (Rudolph and Goins, 1991) found that the phase transition temperatures of DPPC increase with increasing concentration of betaine. They

studied betaine at 0, 1, 2 and 3 M, observing a linear increase in the transition temperatures with increasing betaine concentration. They also found that the transition from gel to ripple phase, T_{pre}, was susceptible to a larger increase than the transition from ripple to fluid phase, T_M. Furthermore, if the concentration of betaine is 3 M or higher, then the ripple phase is completely suppressed. Koynova *et al.* attributed this humectant-induced effect to reflect the much lower enthalpy value for the pretransition as compared to the main transition (Koynova et al., 1997).

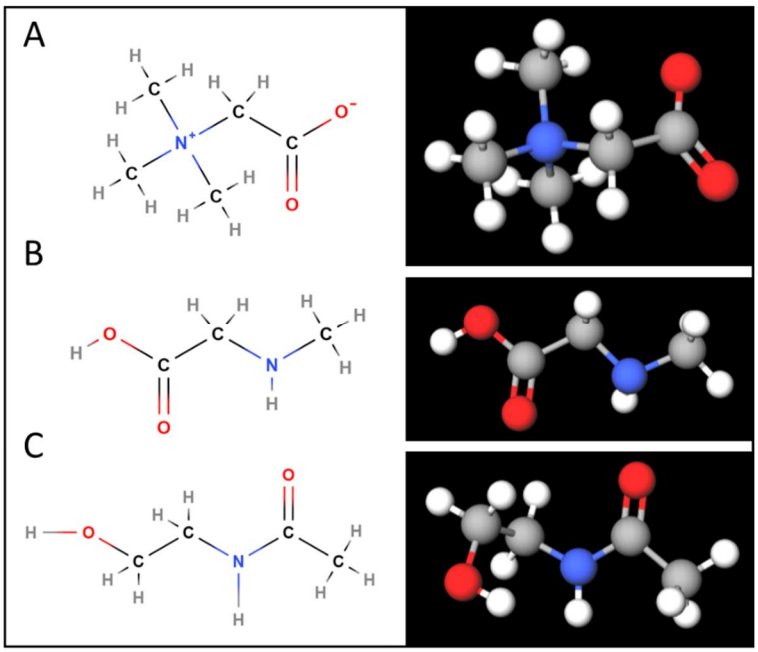

Figure 1. The structure of betaine (A), sarcosine (B) and AMEA (C). All molecular models were made with the online program MolView (http://molview.org/).

Betaine and sarcosine are osmolytes (Kempf and Bremer, 1998; Kumar and Kishore, 2013; Patel and Mehta, 2015; Popova and Busheva, 2001; Takis et al., 2015; Thoppil et al., 2017) having the ability to protect microorganisms against stresses such as dehydration, as well as acting as cryoprotectants. Betaine is also an effective protein stabiliser (Hayashi et al., 2007; Thoppil et al., 2017; Venkatesu et al., 2007) working by means of the "preferential exclusion" mechanism (Moelbert et al., 2004), whereby betaine will be excluded from the protein hydration sphere or protein surface in solution, therefore resulting in a water enriched environment near the protein surface and eliminating any unfavourable interactions between betaine and the protein.

Furthermore, betaine is effective in maintaining membrane integrity and retention of water within the cell (Jolivet et al., 1982; Thoppil et al., 2017), as well as being a methyl donor in

biological functions such as converting homocysteine to methionine (Patel and Mehta, 2015; Thoppil et al., 2017) and evidence on its role in the human health and possible ability to improve athletic performance has been published (Lever and Slow, 2010). Sarcosine has many similar traits as betaine due to its similar chemical nature. In addition to being an osmolyte, sarcosine has shown evidence for improving the memory of patients with schizophrenia (Sharma et al., 2013) and is also found to accelerate the rate of photosynthesis (Chaudhari et al., 2005).

The mechanism by which humectants interact with the lipid bilayer remains in question. Rudolph *et al.* (Rudolph et al., 1986) presented three possible interaction mechanisms for betaine with a lipid bilayer: (i) betaine interacts directly with the hydrocarbon chains, (ii) betaine alters the long range order of water near the polar residues of the lipid, leading to changes in the spacing between the headgroups and (iii) betaine forms coordinate linkages with either the polar headgroups or their hydration sphere, leading to changes in the packing density of the headgroups. The first hypothesis seems rather unlikely as betaine is hydrophilic and a known kosmotrope. However, the authors were not able to attribute their observed results to either hypothesis (ii) or (iii), therefore suggesting that there is a possible combination of mechanisms for interaction. There are a growing number of studies (Anchordoguy et al., 1987; Bruździak et al., 2013; Smiatek et al., 2013) supporting hypothesis (ii), a preferential exclusion mechanism (in concurrence to betaine being an effective protein stabiliser) by which the betaine does not interact with the lipid bilayer directly.

This study explored the effects of humectants on DPPC membranes in further detail, including for the first time at much lower concentrations than previous studies, by using a combination of X-ray scattering and differential scanning calorimetry (DSC). These techniques enabled us to focus on the nanostructural effects of humectants on the DPPC bilayer as well as tracking the thermal changes, thereby providing further insights into the interaction between humectants and DPPC bilayers.

2. Materials and Methods

2.1 Materials

DPPC was purchased from Avanti Polar Lipids, Inc. (Alabaster, U.S.) and used without further purification. Betaine was purchased from Amino GmbH (Frellstedt, Germany), sarcosine was purchased from Chengda (China) and AMEA from Croda (Goole, U.K.). All samples were hydrated with filtered MilliQ water.

2.2 Sample Preparation

Multilamellar vesicles were prepared by the following method. DPPC was dissolved in chloroform/methanol (2:1 respectively) solvent. Aqueous solutions of each humectant were made with filtered milliQ water at the appropriate concentrations. To guarantee the equilibrium distribution of humectants, both in the excess of water and the interlamellar water regions in the liposomal dispersions, we applied a solvent exchange method before making dry lipid films. Briefly, the aqueous solution was added to the DPPC dissolved in chloroform/methanol, resulting in a concentration of DPPC 5 wt. %. The mixture was then heated to 55 °C for 5 minutes, vortexed and placed under vacuum for 15 minutes at room temperature. This procedure was repeated three times, and then the water and the remaining organic solvent was evaporated in a vacuum oven for a minimum duration of 24 h at 2×10^{-1} mbar at room temperature, ensuring that all traces of the solvent were removed. The sample was then rehydrated with filtered MilliQ water, adjusting the DPPC concentration back to 5 wt. %. Finally, the sample was heated for ten times to 55 °C for 5 minutes and vortexed 1-2 minutes, ensuring a homogenous dispersion. Before carrying out the experiments, the samples were left in the fridge at 4 °C overnight. Systematic thin layer chromatography tests on silica gel plates 60 (Merck, Darmstadt, Germany) gave normal results. We note, even with increasing the total incubation time at 55 °C to 4 hours total, no traces of hydrolysis products were visible. The solvent used was chloroform/methanol/water (65/25/4).

2.3 X-ray Scattering Set-Up

Both small- and wide- angle x-ray scattering, SAXS and WAXS, was performed using a SAXSPACE instrument (Anton Paar GmbH, Graz, Austria) equipped with a sealed-tube Cu-anode operating at 40 kV and 50 mA ($\lambda = 0.154$ nm). The 1D scattering patterns were recorded with a Mythen micro-strip X-ray detector (Dectris Ltd, Baden, Switzerland). For the SAXS and WAXS experiments the high-resolution mode was chosen, allowing the detection range to

be from a minimum scattering vector of q_{min} = 0.05 nm^{-1} to q_{max} = 18 nm^{-1} ($q = (4\pi/\lambda)\sin\theta$, where 2θ is the scattering angle. The samples were loaded in 1.5 mm diameter quartz capillaries and were then placed into the temperature-controlled sample stage with Peltier elements installed (TCStage 150, Anton Paar, Graz, Austria). Temperature scans were run from 25 °C to 51 °C at 2 °C intervals with 30 minutes exposure. Between temperatures 40 °C to 45 °C the exposure intervals were reduced to 0.5 °C. The temperature was held for 10 minutes before X-ray exposure.

2.4 Data Reduction

SAXS and WAXS data were obtained for the empty capillary and for the capillary filled with the relevant humectant concentration solution at 25 °C with 30-minute exposures. The position of the primary beam was corrected using SAXStreat software (Anton Paar, Graz, Austria) and the intensity of the primary beam was normalised for all data using SAXSQuant software (Anton Paar, Graz, Austria). Then subtraction of the empty capillary and aqueous solution was performed.

2.5 Calculating Electron Density Profiles

For the gel phase, the Fourier transform method was adopted (Li et al., 2017) where briefly, fitting of each peak is performed before being used in the following equation:

$$\rho(x) = \sum_{h=1}^{h=max} \pm F_h \cos\left(\frac{2\pi x h}{d}\right) \quad (1)$$

where F_h is the form factor, see Equation 2, and x is the distance in real space.

$$F_h = \sqrt{I_h \cdot h} \quad (2)$$

The intensity, I_h, is hereby identified as the peak area of the Bragg peak and is multiplied with Miller index, h, alongside considering the Lorentzian correction (Warren, 1969). The phases of each form factor are well known in literature (Wiener et al.) as - - + - and can be applied to the obtained F_h values, which can then be plotted against x to generate an EDP. Structural parameters such as d (lattice) spacing, head-to-headgroup thickness, d_{HH}, and water layer thickness, d_W, are obtained directly from the generated EDPs.

For the fluid phase, a global fitting method according to the modified Caillé theory was adopted to account for the lattice disorder, which is well described in (Pabst et al., 2003). The bilayer model used has been described previously (Rappolt, 2010). Structural parameters as described above are obtained directly from the fits to the scattered intensities. Mean fluctuations of the

membrane position, σ, can derived from the Caillé parameter, η, which is obtained directly from the fit (Petrache et al., 1998):

$$\sigma = \sqrt{\eta}\frac{d}{\pi} \tag{3}$$

where d is the d spacing.

2.5 Calculating the Area per Lipid Chain

The area per lipid chain, A_C, for the gel phase and the fluid phase was calculated from the WAXS recorded data. For the gel phase, peak fitting was performed to determine the peak positions and then used in the following equation (Sun et al., 1994):

$$A_{C(gel)} = \frac{d_{20}d_{11}}{\sqrt{1-\left(\frac{d_{11}}{2d_{20}}\right)^2}} \tag{4}$$

Where d_{20} is the corresponding d spacing for the centre of the first peak (q_{20}) and d_{11} is the corresponding d spacing for the centre of the second peak (q_{11}), see Figure S1 in the Supporting Information (SI). For the fluid phase, a Lorentzian peak fit of the WAXS data at T_M + 2 °C was executed to quantify the short-range interchain correlation peak position and its correlation length (Hub et al., 2007; Spaar and Salditt, 2003) in order to evaluate, if the humectants had any accountable influence in the chain packing in the fluid phase.

2.6 Differential Scanning Calorimetry

Differential scanning calorimetry (DSC) was conducted using a DSC 8000 (PerkinElmer, Seer Green, U.K.) which is calibrated with both indium and zinc standards and installed with a cooling system, Intracooler 2 for DSC 8X00 (PolyScience, Illinois, U.S.A.). Each sample is measured from 25 to 50 °C at 1 °C/min scan rate and all DSC scans were repeated three times. Microcalorimetric scans of diluted dispersions showed highly cooperative chain melting phase transition ($\Delta T_{1/2}$ < 0.3 °C for pure DPPC), at the same melting temperature in agreement with the published values (Albon and Sturtevant, 1978; Jørgensen, 1995), thus providing another guarantee that the lipid purity after sample preparation corresponds to the claimed one of 99%.

Phase transition temperatures are taken from the DSC results as the maximum of the turnover peak. The enthalpy values of both pre- and main transition were determined from the given peak area, and the FWHM, i.e., $\Delta T_{1/2}$, are given for the main transition only. For pure DPPC an example DSC curve and the peak fitting using Gaussian distributions are shown in Figure S2 in the SI.

3. Results

3.1 Thermotropic Changes

When immersed in excess water, DPPC will self-assemble in to lyotropic lamellar phases. Depending on the temperature, three phases are observed from 25 to 50 °C, the lamellar gel phase, $L_{\beta'}$, the stable ripple phase, $P_{\beta'}$, and the lamellar fluid phase, L_{α}. The transition from gel phase to ripple phase is called the pre-transition temperature, T_{pre}, which occurs at 35-36 °C (Koynova and Caffrey, 1998). The transition from ripple to fluid phase is called the main transition temperature, T_M, and is observed at 41.5 °C (Koynova and Caffrey, 1998). The DSC results show the influence of the humectants on these two phase transition temperatures of DPPC (Figure 2A-C and

Table **1**). The results agree with previous studies (Rudolph and Goins, 1991), as T_{pre} is affected more than T_M, i.e., dT_{pre}/dc is greater than dT_M/dc.

However, the inclusion of lower concentrations of betaine (< 1 M) in this study, shows that the increase in transition temperatures is not linear over the entire concentration range as stated earlier (Rudolph et al., 1986). In fact, at very low concentrations of 0.05 and 0.15 M betaine (which Rudolph and Goins had not investigated), the phase transition temperature is lowered for both T_{pre} and T_M. This behaviour is also observed with sarcosine. The addition of AMEA lowers T_{pre} with increasing concentrations while having no effect on T_M. This difference in behaviour of AMEA on DPPC compared to betaine and sarcosine is unexpected with respect to its equivalent role as a humectant.

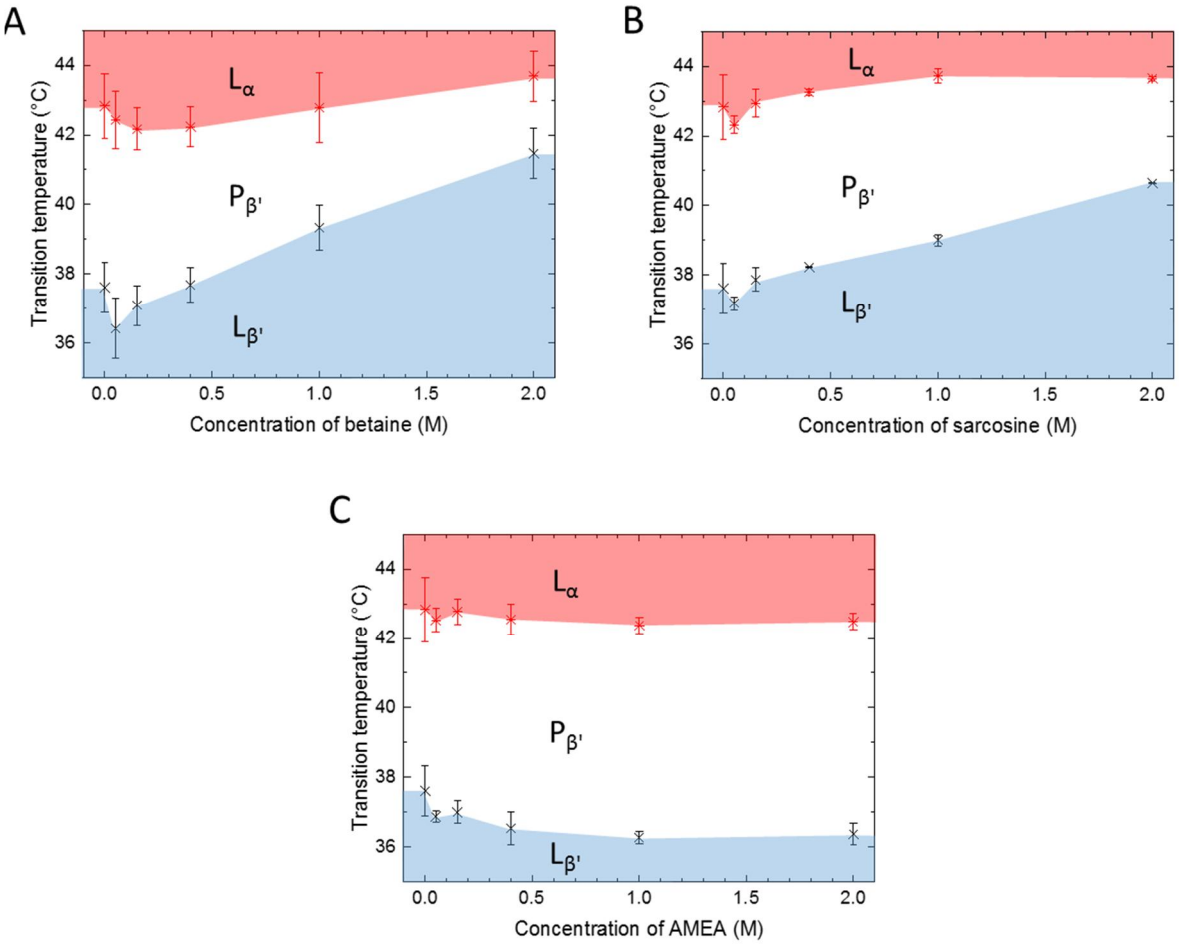

Figure 2: Phase behaviour DPPC under the influence of different humectants. The phase diagrams of fully hydrated DPPC with A) betaine, B) sarcosine and C) AMEA.

The enthalpy values for both transitions have been determined and are shown in Table 1. The general trend of transitions temperatures for betaine and sarcosine increases, while the

corresponding enthalpy values tend to drop with the humectant concentration. With AMEA, the enthalpy trends follow the transition temperature trend by both decreasing with increasing concentration.

Table 1: The phase transition temperature and enthalpy values of fully hydrated DPPC with betaine, sarcosine and AMEA.

Concentration of Betaine (M)	Pre-transition		Main transition	
	Temperature [a] (°C)	Enthalpy (kcal/mol)	Temperature [b]/$\Delta T_{1/2}$ (°C)	Enthalpy (kcal/mol)
0.00	36.3	1.33±0.13	41.5/ 0.28	7.52±0.38
0.05	35.1	0.90±0.09	41.1/ 0.28	6.97±0.35
0.15	35.8	1.28±0.13	40.9/ 0.31	7.90±0.40
0.40	36.4	1.15±0.11	40.9/ 0.31	7.30±0.36
1.00	38.0	0.90±0.09	41.5/ 0.31	7.17±0.36
2.00	40.2	0.80±0.08	42.4/ 0.44	7.81±0.39
Concentration of Sarcosine (M)	**Pre-transition**		**Main transition**	
	Temperature [a] (°C)	**Enthalpy (kcal/mol)**	**Temperature [b]/$\Delta T_{1/2}$ (°C)**	**Enthalpy (kcal/mol)**
0.00	36.3	1.33±0.13	41.5/ 0.28	7.52±0.38
0.05	35.9	1.01±0.10	41.0/ 0.40	7.70±0.39
0.15	36.6	1.09±0.11	41.7/ 0.35	7.99±0.40
0.40	36.9	0.76±0.08	42.0/ 0.41	5.85±0.29
1.00	37.7	0.76±0.08	42.4/ 0.54	6.30±0.31
2.00	39.4	0.83±0.08	42.4/ 1.19	5.73±0.29
Concentration of AMEA (M)	**Pre-transition**		**Main transition**	
	Temperature [a] (°C)	**Enthalpy (kcal/mol)**	**Temperature [b]/$\Delta T_{1/2}$ (°C)**	**Enthalpy (kcal/mol)**
0.00	36.3	1.33±0.13	41.5/ 0.28	7.52±0.38
0.05	35.6	0.91±0.09	41.2/ 0.40	8.74±0.43
0.15	35.7	0.98±0.10	41.5/ 0.44	7.39±0.37
0.40	35.3	1.05±0.11	41.3/ 0.41	7.29±0.36
1.00	35.0	1.33±0.13	41.1/ 0.39	6.53±0.33
2.00	35.1	0.61±0.06	41.2/ 0.50	5.70±0.29

[a] The pretransition temperatures were measured within errors of 0.3 to 0.4 °C and [b] the main transition temperatures were determined within errors of 0.05 to 0.15 °C (see Fig. 2).

3.2 Structural Changes

Changes in the nanostructure of DPPC was monitored by X-ray scattering experiments. Determined electron density profiles, EDPs, from the SAXS results reveal various structural information (Figure 3A). Here the head group to head group distance, d_{HH}, and the water layer thickness, d_W, are displayed, where $d = d_{HH} + d_W$. The influence of the humectants on the bilayer for the gel phase is shown in Figure 3B-D. The decrease in d_W dominates over the slight increase in d_{HH}, resulting in an overall increase in d. Clearly, all three humectants do behave as typical kosmotropes, i.e., by partial dehydration of the lipid/water interface, the bilayers are

further stabilized (seen by the slight increase of d_{HH}). Consequently, an enhanced bending rigidity of the bilayers is expected leading to a decrease in repulsive undulation forces, and hence, to a contribution in the decrease in the inter-bilayer distance, d_W, with increasing concentration of humectant. Noteworthy, this general trend was observed for all three humectants in the gel-phase with no clear indication to which humectant has the greatest effect on the DPPC membranes.

Similar trends were expected for the influence of humectants on the bilayer structure in the fluid lamellar phase above T_M. All recorded diffraction patterns have been fitted with a global fitting method according to the modified Caillé theory (see Material and Methods Section), which is displayed in Figure S3 in the SI for all betaine samples. However, no clear trend could be found within fitting errors for the bilayer thickness or for the bilayer undulations, see Figure S4. In other words, independent of the concentration of humectant, parameters d_{HH} and the Caillé parameter, η, remained practically constant over the range from 0 to 2M (note, the fitting parameter η is proportional to the square root of the membrane displacement, σ - see Equation 3). Nevertheless, like with the gel-phase findings, most significant changes were recorded in the water layer thickness, d_W, for the fluid phase. For the highest concentrations, a clear thinning of d_W was displayed for betaine and sarcosine, e.g., at 2M betaine d_W decreased by about 0.35 nm (see Figure S4B in the SI). This trend of de-swelling of the multilamellar vesicles in the presence of betaine and sarcosine is further confirmed by the clear drop in the lattice parameter, d (Figure S4C).

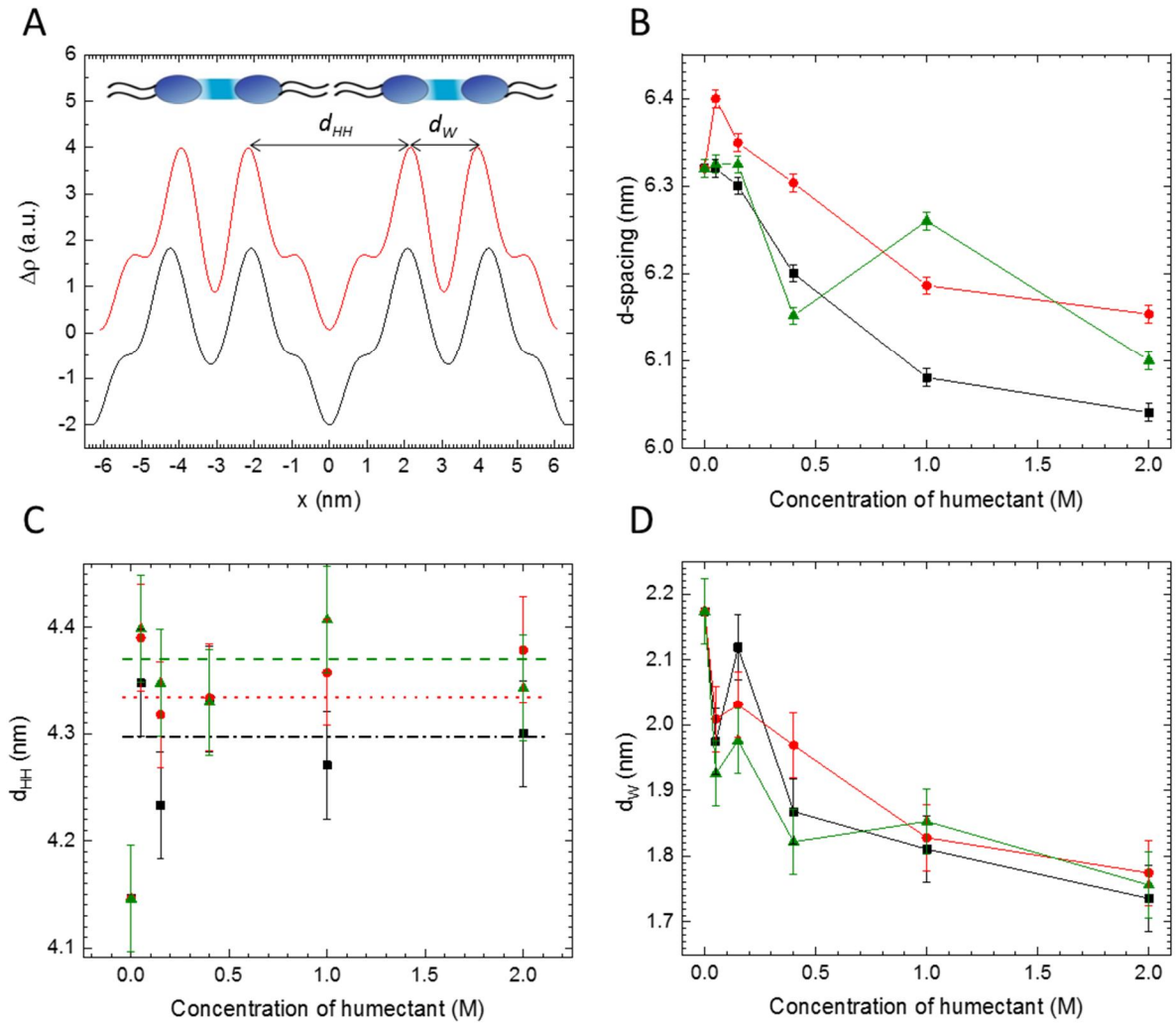

Figure 3: Structural analysis of DPPC bilayers under the influence of humectants in the $L_{\beta'}$ phase. A) Electron density profiles of bilayers of pure DPPC (black line) and DPPC plus 2M betaine (red line) illustrate clearly an increase of the bilayer thickness with concomitant decrease in the water layer thickness. Change of the *d*-spacing (B) (note, horizontal lines display the average d_{HH} values in the presence of humectant), d_{HH} (C) and d_W (D) are shown for DPPC with increasing concentration of humectants (betaine –black, sarcosine – red and AMEA – green).

The results from the WAXS investigations offer additional insights. WAXS contour plots shown in Figure 4, demonstrate clearly the main phase transition temperature reflected by its short spacings. At T_M the diffraction peaks arising from the packing of the chains in the gel-phase vanish (dominant short spacing is 0.41 nm or q = 15.3 nm^{-1}), leaving only a diffuse broad scattering peak in the fluid phase. This diffuse scattering centred at about $q = 2\pi/0.46$ nm = 13.6 nm^{-1} originates from the short range order of the hydrocarbon chains (Hub et al., 2007).

The position and width of this peak does not change (within errors) as a function of humectant concentration.

The transition temperatures of the pre-transition and the main-transition deduced from the WAXS-measurements compare well to our DSC-results (cp. Table 1). As shown, the influence of increasing betaine's concentration leads to a reduction in the pre- to main-transition interval (cp. Figure 2A). Finally, having scaled the contour plots to display the same maximum intensity in the fluid phase (colour-coded yellow), it is evident, that particularly the lower betaine concentrations (50 mM and 0.15 M), display far lower short-spacing intensities in the gel-phase regime, when compared to the pure DPPC dispersion. That is, the effective number and/or domain size of fatty acid crystallites, contributing to the gel-phase peak intensities, is reduced. Remarkably, this observation coincides with the counterintuitive reduction in the pre- as well as main-transition temperatures in this lower concentration regime (cp. Figure 2A and discussion section 4.1).

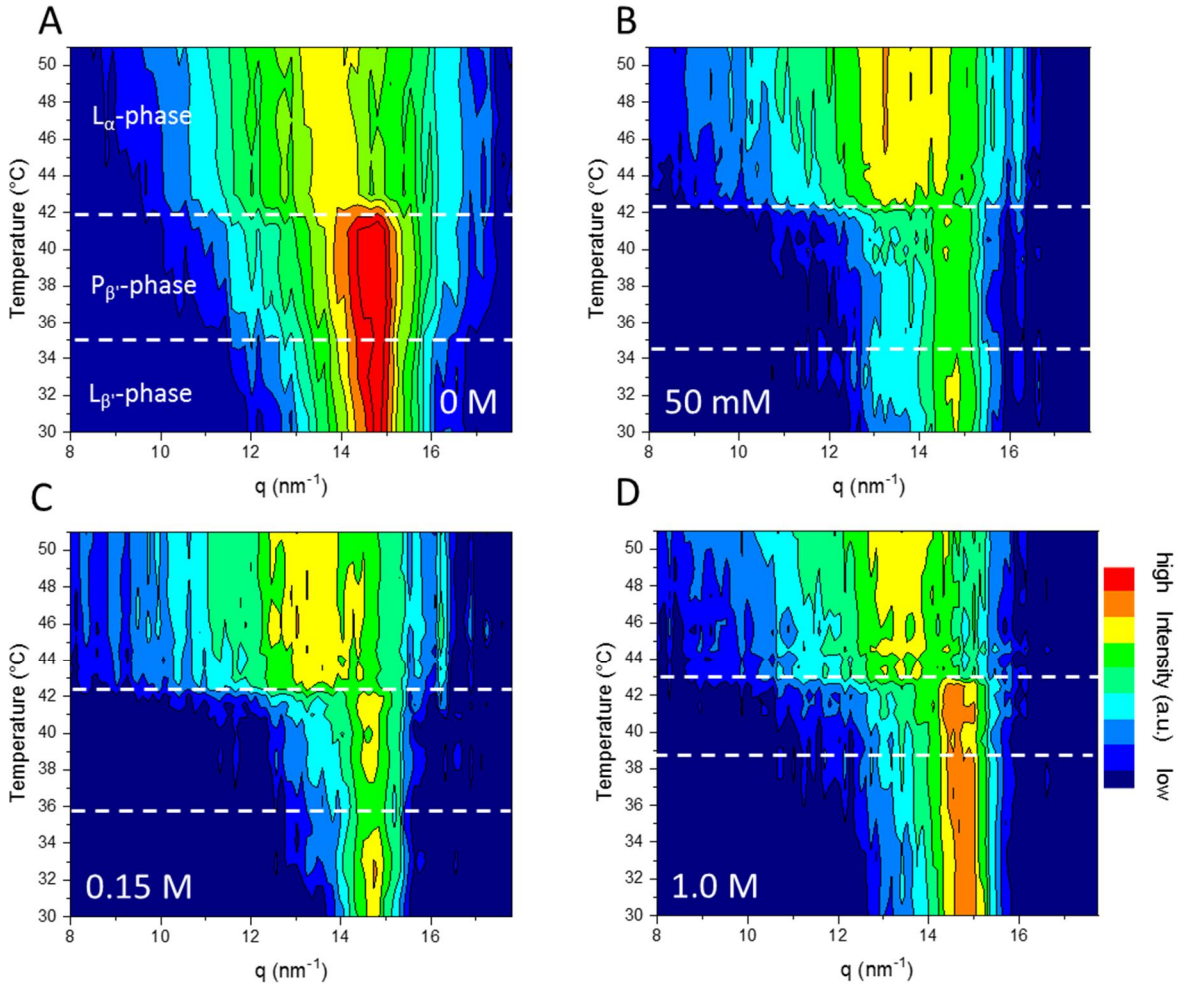

Figure 4: Contour plots of the WAXS patterns as a function of temperature. A) Pure DPPC, B) DPPC with 50 mM betaine, C) with 0.15 M betaine and D) 1.00 M betaine.

The change in area per lipid chain, A_C, has been calculated for the $L_{\beta'}$ phase (Figure 5A). A slight decrease in A_C is observed for all humectants, again supporting the view of slightly solidifying bilayers under the influence of humectants. On the other hand, a slight decrease in the area per chain should lead to a greater mismatch between the projected chain and headgroup area. Thus, a rearrangement of the headgroup packing with higher density would be plausible (we shall return to this point later in our discussion on possible van der Waals force alterations). Lastly, taking a closer look at the diffraction pattern observed for high AMEA concentrations at 25 °C, we observe a change in the chain packing, since the intensity ratio between q_{20} and q_{11} changes (see Figure S5 in the SI). At 1 M AMEA, the peak intensities of the q_{20} peak and q_{11} peak are almost equal (note, at 0 M the q_{20} peak is clearly the most intense peak as one would expect). Finally, at 2 M AMEA the q_{11} peak is even more intense as the q_{20} diffraction peak (Figure 5B). This change in electron density contrast for the short spacings is not observed for betaine and sarcosine, where the relative peak intensities remain nearly the same at all concentrations with q_{20} remaining the dominant peak (Figure S5). This reaffirms the above observations that betaine and sarcosine behave alike, also with respect to the lipid chain packing, whereas AMEA underlines its outsider role with displaying a q_{20} : q_{11} ratio < 1 at concentrations greater than 1 M, i.e., inducing an electron density contrast variation with respect to the lipid packing (Figure 5B).

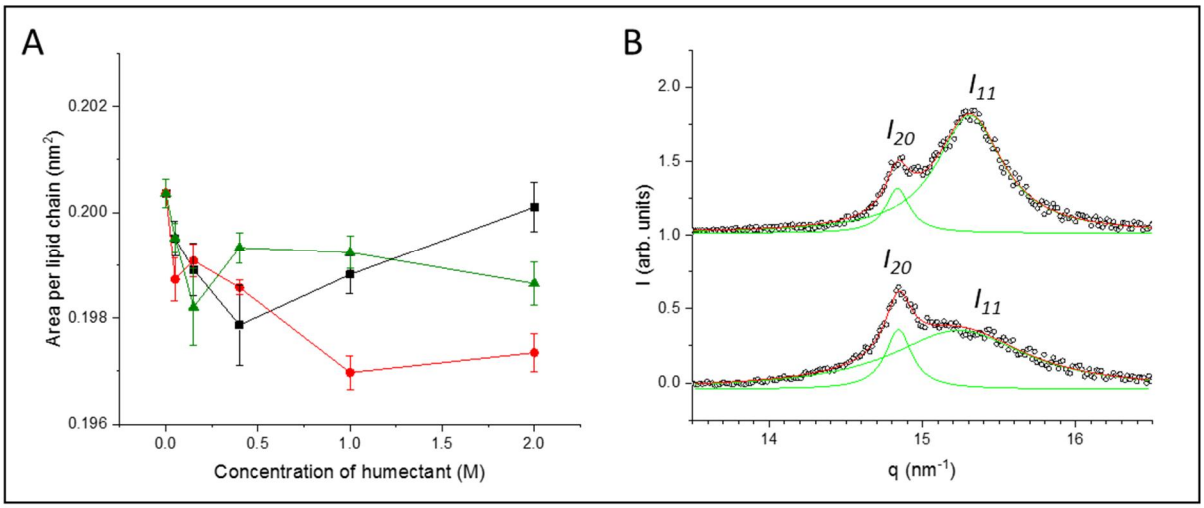

Figure 5: The change in area per lipid chain for A) the gel phase at 25 °C (betaine – black, sarcosine – red and AMEA – green) and B) WAXS pattern reflecting the chain packing in the gel-phase of DPPC (bottom) and DPPC with 2M AMEA (top). For pure DPPC the calculated area per chain compares very well with literature values (Sun et al., 1994). Note, for better achieving counting statistics, WAXS pattern have been averaged from 25 to 33 °C.

4. Discussion

4.1 Thermotropic Changes

Our betaine results are, in general, in agreement with previous findings (Rudolph and Goins, 1991), however, the additional investigation of lower concentrations (< 1 M) of betaine show that the transition temperatures do not increase linearly over the entire concentration regime. At low concentrations of about 0.05 M, betaine actually decreases T_{pre}, which is observed for sarcosine as well but to a smaller extent. This suggests that the humectants at these lower concentrations might only partially deplete water from the lipid/water interface, resulting in coexisting domains of partially dehydrated and fully hydrated areas, respectively. This proposed inhomogeneity of interfacial hydration could in turn lead to disorder at the membrane interface at low humectant concentrations. We note, while the number of waters per lipid do only slightly decrease with the humectant concentration, the number of humectants per lipid is rather low up 0.4 M (0.03 to 0.22), and the proposed full water depletion effect of water is reached at a humectant per lipid ratio of about 0.5 to 1.0 (see Table 2). Thus, we suggest that the depletion effect at higher concentrations leads to a homogenous dehydration of the membranes, with an observed increasing ordering effect of the bilayers. Secondly, it is important to note, that the water-depletion effect by humectants is not accompanied by any traceable effect of osmosis. All samples were prepared to ensure the equilibrium distribution of humectants in the excess of water and interlamellar water regions, respectively (see Materials and Methods section). This is further confirmed by the SAXS diffraction pattern not displaying any phase separation into water-rich and water-poor MLVs, as will occur under osmotic conditions caused by strong solute concentration variations within the interlamellar regions (Rappolt et al., 2001; Rappolt et al., 1998).

For the further discussion of the thermotropic results, we briefly introduce the thermodynamic theory for the effect of kosmotropic and chaotropic solutes on the phases transition of lipid/water systems, that has been presented in great detail by Koynova, Brankov and Tenchov (Koynova et al., 1997). This thermodynamic approach considers the manifestation of the underlying microscopic interactions in terms of purely macroscopic, measurable thermodynamic quantities such as changed water and solute concentrations in the lipid phase and culminates in a simple equation for the phase transition temperatures, T_{tr}, changes under the influence of changing solute concentrations, c:

$$\frac{dT_{tr}}{dc} = \frac{R\,T_{tr}^2}{\Delta H}\,(n_W' - n_W'')\left(1 - \frac{c_L}{c}\right) \qquad (6)$$

where dT_{tr}/dc is the solute dependent change of the transition temperature (humectant in this case), R is the gas constant, ΔH is the transition enthalpy, n_W is the fraction of interlamellar water per lipid, where prime and double-prime denote the high and low temperature phases, respectively, c_L is the solute concentration in the interlamellar water region and c is the solute concentration in bulk (excess water region). We note that this thermodynamic model assumes that first-order phase transitions are given, and secondly, that the solute concentration in the interlamellar regions are the same in the high and low temperature phases (note, if needed the difference of interlamellar humectant concentrations can be accounted for; see (Koynova et al., 1997).

Returning to our discussion, the observed thermotropic effect of betaine and sarcosine on fully hydrated DPPC show generally that dT_{pre}/dc is greater than dT_M/dc. This agrees with this theory, because the given enthalpies of the pretransition of are about seven-fold smaller than the main transition (note, ΔH is given in the denominator of the first term). The second term (n_W'- n_W'') is for both transitions positive. Note, n_W is for the $L_{\beta'}$ phase about 14, for L_α phase about 30 (see Table 2) and for the $P_{\beta'}$ phase about 23 (De Vries et al., 2005). This second term n_W'- n_W'' does not alter much between betaine, sarcosine and AMEA, it also does not vary significantly as a function of humectant concentration, since all n_W values decrease only slightly with c_L. The betaine data in Table 2 give a good estimation on how Equation 6 is influenced by this term. The third term of the equation, (1 - c_L/c) describes the influence of the unequal humectant concentration between bulk and interlamellar water. As outlined before, kosmotropes dehydrate the lipid/water interface, and as a consequence, $c_L < c$. That is, the overall value for dT_{tr}/dc is expected to be positive, as clearly seen for betaine and sarcosine.

For AMEA instead, a decrease in T_{pre} and T_M is observed over the entire concentration interval (Figure 2). This difference in behaviour between AMEA and betaine or sarcosine suggests that AMEA interacts differently with DPPC. While the enthalpic term and second interlamellar water term are very similar, maybe c_L for AMEA is enhanced and/or a direct macroscopic interaction of AMEA with the lipid/water interface are not accounted by this thermodynamic model.

In previous studies, there are conflicting conclusions on whether betaine or sarcosine is the more effective osmolyte for protein stabilisation (Anchordoguy et al., 1987; Bruździak et al., 2013; Gopal and Ahluwalia, 1993; Thoppil et al., 2017). In this study, the effect of betaine and sarcosine on hydrated DPPC is also inconclusive as to which humectant has a larger effect. For T_{pre} betaine has a slightly larger effect on both the temperature and enthalpy, where 2 M betaine

leads to a 3.9 °C increase compared to a smaller increase of 3.0 °C for 2 M sarcosine. The difference in enthalpy values is smaller, but nonetheless, betaine has a larger effect of decreasing the enthalpy of T_{pre} by 0.53 kcal/mol for 2 M betaine compared to a decrease of 0.50 kcal/mol for 2 M sarcosine. Therefore, it gives reasons to conclude that betaine has a slightly larger effect on T_{pre}. However, when comparing the effects on T_M, both betaine and sarcosine increase the transition temperature by 0.8 °C at 2 M concentration. When the enthalpy effect is compared, it is marginally changed by 2 M betaine with a slight increase of 0.29 kcal/mol. Whereas 2 M sarcosine decreases the enthalpy by 1.79 kcal/mol. Apart from these marginal differences, both betaine and sarcosine do display very similar phase diagrams (Figure 2A and B), in which the lamellar gel phase is increasingly stabilised with increasing humectant concentration.

Table 2: Number of water and betaine per lipid at 25 °C deduced from the area per lipid, A_L, and water layer thickness, d_W with $V_W = A_L \cdot d_W/2$.

Concentration of Betaine	A_L (nm^2)	d_W (nm)	V_W per lipid (nm^3)	n_W [a] per lipid	Betaine per lipid [b]
0.00	0.400	2.17	0.436	14.5	0.0000
0.05	0.399	1.97	0.394	13.1	<0.01
0.15	0.398	2.12	0.422	14.1	<0.03
0.40	0.396	1.87	0.370	12.3	<0.09
1.00	0.398	1.81	0.360	12.0	<0.22
2.00	0.404	1.74	0.351	11.7	<0.42

[a] The number of water molecules, n_W, per lipid was calculated from the water volume, V_W, per lipid divided the volume of one water molecule, i.e., 0.03 nm^3. [b] This estimate is based on the oversimplification that the concentration of betaine is the same in excess of water as in the interlamellar water regions.

4.2 Structural Changes

The SAXS results for the both the gel phase and the fluid phase shows that the addition of any of the three humectants leads to a decrease in d_W and a slight increase in d_{HH}. Thus, overall a decrease in the d spacing is observed with increasing concentration of humectant. The slight increase in d_{HH} along with the decrease in d_W suggests that the Helfrich undulations are reduced with addition of humectant, caused by a partial dehydration effect on the lipid/water interface (Parsegian, 1967). Consequently, an enhanced bending rigidity of the bilayers is expected, leading to a decrease in repulsive undulation forces, and hence contributing to the decrease in the inter-bilayer distance, d_W, with increasing concentration of humectant. Assuming the

Young modulus, E, will not change significantly under the influence of the humectants, we can estimate the change in bending modulus K_C as a function of the bilayer thickness d_{HH}. With $K_C = E\, d_{HH}^3/9$ and $E = 116\ 10^6$ Pa (Et-Thakafy et al., 2017), we get for pure DPPC, DPPC plus 2 M betaine, 2 M sarcosine and 2 M AMEA, respectively, values of K_C of $9.2\ 10^{-19}$, $10.2\ 10^{-19}$, $10.4\ 10^{-19}$ and $10.7\ 10^{-19}$ J. Hence, the Helfrich undulation forces being indirect proportional to K_C, are expected to decay in the order of 10-15% under the influence of humectants (cp. Figure 3C). A reduction to the repulsive forces would suggest an increase in the order of the bilayers, which agrees with the interpretation of the thermal results where an increase in order of the system for betaine and sarcosine is observed. Moreover, a slight reduction of the area per chain, A_C, in the gel phase upon addition of humectant is further evidence that the bilayer becomes more ordered.

On the other hand, one must also consider possible variations of van der Waals interaction between the bilayers, where the same effect on the inter-bilayer distance may be achieved, if the van der Waals forces were increased. Importantly, the Hamaker constant depends on the static dielectric permittivity of the intermediate medium (see chapter 13 in (Israelachvili, 2011)). The dielectric permittivity of water depends on the concentration of water, and is therefore reduced, when molecules with smaller dipole moments are added. Such an effect has been for instance observed, when adding sodium chloride to water ((Gongadze et al., 2018)). The dielectric permittivity drops with the kosmotrope concentration and hence the Hamaker constant increases. The dielectric permittivity may be additionally decreased due to a denser packing of the lipid headgroups in the gel-phase (see results section 3.2), since this increases the effective surface charge densities in the headgroup region of the zwitterionic layer. Such a decrease in permittivity was shown to contribute to the increase of the Hamaker constant in theoretical model calculations (Gongadze et al., 2014). In this respect, betaine, sarcosine and AMEA display very similar effects on the thinning of d_W (Figure 3D), most probably caused by dominantly by an increase of the van der Waals forces. Last, we do not consider any significant influence of hydration forces, since they become dominant at interlamellar distances of a few water molecule diameters only.

Despite the same nanostructural trends observed in the fluid phase compared to the gel phase, i.e., a decrease in d_W and overall decrease in d, no trend was determined from the fittings of the fluid phase with respect to the Caillé parameter, η. The observed nanostructural changes led to the expectation of a decrease in η with increasing humectant concentration. It might be that

minor structural trends in the fluid bilayer are too small to be picked up due to the chosen simple two Gaussian model for the bilayer (i.e., d_{HH} varies in an interval of 3.65 to 3.90 nm without clear trend, and η from 0.08 to 0.12, see Figure S4A and S4D in SI). However big or small the changes in the mechanics of the fluid bilayers might be, the above arguments on influence of the humectants on the Hamaker constant remain valid also in the L_α-phase. A reduction the static dielectric permittivity by the presence of kosmotropes is expected to enhance the van der Waals forces, and hence explains the observed decrease of the interlamellar water thickness also here.

Calculating the chain area, A_C, for the gel phase provided insights into changes in packing density of the lipid chains. This has confirmed the ordering effect of all three humectants on the DPPC gel-phase. However, the observed q_{20}:q_{11} peak ratio changes in the WAXS at high concentration of AMEA, indicates a change in the molecular electron contrast that might be caused by AMEA also partitioning in to the lipid headgroup interface, and therefore giving a possible microscopic explanation for contributing to the lowering of T_{pre} and T_M. As this is not observed at the higher concentrations of betaine and sarcosine, it is evidence to support the preferential exclusion mechanism of betaine and sarcosine (Bruździak et al., 2013; Thoppil et al., 2017). This mechanism of interaction would support the second proposed mechanism by Rudolph *et al*. (Rudolph et al., 1986), whereby the humectant affects the long range order of the water near the polar residues, but does not interact directly with the lipid bilayer.

5. Conclusion

The humectants betaine, sarcosine and AMEA, have been studied for their influence on the structure and thermotropic behaviour of fully hydrated DPPC. Overall betaine influences DPPC the most, by having the larger effect on T_{pre} and on the nanostructure of DPPC bilayers over sarcosine. Finally, betaine and sarcosine interact with DPPC bilayer via a similar depletion mechanism of water from the lipid/water interface. Notably, at low humectant concentrations the relatively weak depletion of interfacial water leads to an intermittent disorder of the membranes, while at higher concentrations a subsequent ordering of the membrane is eminent. Furthermore, AMEA leads to an increase of bilayer order at high concentrations, however, it affects DPPC bilayers in a different manner, since it additionally interacts with the polar lipid interface.

To pinpoint the location of the humectants within the hydrated DPPC bilayers, neutron scattering studies combined with molecular dynamics simulation would provide further insight as to their kosmotropic behaviour at a molecular level. In addition, FT-IR spectroscopy studies could enable us to investigate specific chemical interactions by change in bond vibrational frequencies, resulting from the addition of humectants.

Acknowledgements

The authors would also like to acknowledge the great help of Dr Amin Sadeghpour Dilmaghani and Dr Arwen Tyler. We are also grateful to Prof Aleš Iglič for pointing us in the right direction, concerning possible changes of the Hamaker constant in dependence of the static dielectric permittivity. Finally, we would like to thank the EPSRC funded Soft Matter and Functional Interfaces Centre for Doctoral Training (SOFI CDT), grant code EP/L015536/1, and also to GSK for their funding and support.

References

Ahmadi, D., Ledder, R., Mahmoudi, N., Li, P., Tellam, J., Robinson, D., Heenan, R.K., Smith, P., Lorenz, C.D., Barlow, D.J., Lawrence, M.J., 2021. Supramolecular architecture of a multi-component biomimetic lipid barrier formulation. Journal of Colloid and Interface Science 587, 597-612.

Ahmadi, D., Mahmoudi, N., Li, P., Ma, K., Doutch, J., Foglia, F., Heenan, R.K., Barlow, D., Lawrence, M.J., 2020. Revealing the Hidden Details of Nanostructure in a Pharmaceutical Cream. Scientific Reports 10, 4082.

Akutsu, H., 2020. Structure and dynamics of phospholipids in membranes elucidated by combined use of NMR and vibrational spectroscopies. Biochimica et Biophysica Acta - Biomembranes 1862.

Al-Muhtaseb, A.H., McMinn, W.A.M., Magee, T.R.A., 2002. Moisture sorption isotherm characteristics of food products: A review. Food and Bioproducts Processing: Transactions of the Institution of of Chemical Engineers, Part C 80, 118-128.

Albon, N., Sturtevant, J.M., 1978. Nature of the gel to liquid crystal transition of synthetic phosphatidylcholines. Proc.Natl.Acad.Sci.U.S.A 75, 2258-2260.

Anchordoguy, T.J., Rudolph, A.S., Carpenter, J.F., Crowe, J.H., 1987. Modes of interaction of cryoprotectants with membrane phospholipids during freezing. Cryobiology 24, 324-331.

Bruździak, P., Panuszko, A., Stangret, J., 2013. Influence of Osmolytes on Protein and Water Structure: A Step To Understanding the Mechanism of Protein Stabilization. The Journal of Physical Chemistry B 117, 11502-11508.

Chaudhari, A., Sahu, P.K., Lee, S.L., 2005. Hydrogen bonding interaction in sarcosine-water complex using ab initio and DFT method. Int. J. Quantum Chem. 101, 97-103.

De Vries, A.H., Yefimov, S., Mark, A.E., Marrink, S.J., 2005. Molecular structure of the lecithin ripple phase. Proceedings of the National Academy of Sciences of the United States of America 102, 5392-5396.

de Vringer, T., Joosten, J.G.H., Junginger, H.E., 1987. A study of the gel structure in a nonionic O/W cream by X-ray diffraction and microscopic methods. Colloid and Polymer Science 265, 167-179.

Et-Thakafy, O., Delorme, N., Gaillard, C., Mériadec, C., Artzner, F., Lopez, C., Guyomarch, F., 2017. Mechanical Properties of Membranes Composed of Gel-Phase or Fluid-Phase Phospholipids Probed on Liposomes by Atomic Force Spectroscopy. Langmuir 33, 5117-5126.

Gesslein, B.W., 1999. Humectants in personal care formulation: a practical guide. Cosmetic Science and Technology Series, 95-110.

Gongadze, E., Mesarec, L., Kralj-Iglič, V., Iglič, A., 2018. Asymmetric finite size of ions and orientational ordering of water in electric double layer theory within lattice model. Mini-Reviews in Medicinal Chemistry 18, 1559-1566.

Gongadze, E., Velikonja, A., Perutkova, Š., Kramar, P., Maček-Lebar, A., Kralj-Iglič, V., Iglič, A., 2014. Ions and water molecules in an electrolyte solution in contact with charged and dipolar surfaces. Electrochimica Acta 126, 42-60.

Gopal, S., Ahluwalia, J.C., 1993. Effect of osmoregulatory solutes on the stability of proteins. Journal of the Chemical Society, Faraday Transactions 89, 2769-2774.

Hayashi, Y., Katsumoto, Y., Oshige, I., Ornori, S., Yasuda, A., 2007. Comparative study of urea and betaine solutions by dielectric spectroscopy: Liquid structures of a protein denaturant and stabilizer. J. Phys. Chem. B 111, 11858-11863.

Hub, J.S., Salditt, T., Rheinstädter, M.C., De Groot, B.L., 2007. Short-range order and collective dynamics of DMPC bilayers: A comparison between molecular dynamics simulations, X-ray, and neutron scattering experiments. Biophysical Journal 93, 3156-3168.

Israelachvili, J., 2011. Intermolecular and Surface Forces, 3rd Edition ed. Academic Press, London.

Jolivet, Y., Larher, F., Hamelin, J., 1982. Osmoregulation in halophytic higher plants: The protective effect of glycine betaine against the heat destabilization of membranes. Plant Science Letters 25, 193-201.

Jørgensen, K., 1995. Calorimetric detection of a sub-main transition in long-chain phosphatidylcholine lipid bilayers. Biochim.Biophys.Acta 1240, 111-114.

Kempf, B., Bremer, E., 1998. Uptake and synthesis of compatible solutes as microbial stress responses to high-osmolality environments. Archives of Microbiology 170, 319-330.

Koynova, R., Brankov, J., Tenchov, B., 1997. Modulation of lipid phase behavior by kosmotropic and chaotropic solutes. Experiment and thermodynamic theory. European Biophysics Journal 25, 261-274.

Koynova, R., Caffrey, M., 1998. Phases and phase transitions of the phosphatidylcholines. Biochimica et Biophysica Acta (BBA) - Reviews on Biomembranes 1376, 91-145.

Kumar, N., Kishore, N., 2013. Structure and effect of sarcosine on water and urea by using molecular dynamics simulations: Implications in protein stabilization. Biophys. Chem. 171, 9-15.

Lever, M., Slow, S., 2010. The clinical significance of betaine, an osmolyte with a key role in methyl group metabolism. Clinical Biochemistry 43, 732-744.

Li, N.Y.D., Perutková, Š., Siglic, A., Rappolt, M., 2017. My first electron density map: A beginner's guide to small angle X-ray diffraction. Elektrotehniski Vestnik/Electrotechnical Review 84, 69-75.

Lodén, M., 2003. Role of Topical Emollients and Moisturizers in the Treatment of Dry Skin Barrier Disorders. American Journal of Clinical Dermatology 4, 771-788.

Moelbert, S., Normand, B., De Los Rios, P., 2004. Kosmotropes and chaotropes: modelling preferential exclusion, binding and aggregate stability. Biophys. Chem. 112, 45-57.

Nagle, J.F., Tristram-Nagle, S., 2000. Structure of lipid bilayers. Biochimica Et Biophysica Acta-Reviews on Biomembranes 1469, 159-195.

Nagle, J.F., Zhang, R., Tristram-Nagle, S., Sun, W., Petrache, H.I., Suter, R.M., 1996. X-ray structure determination of fully hydrated L alpha phase dipalmitoylphosphatidylcholine bilayers. Biophysical Journal 70, 1419-1431.

Pabst, G., Amenitsch, H., Kharakoz, D.P., Laggner, P., Rappolt, M., 2004. Structure and fluctuations of phosphatidylcholines in the vicinity of the main phase transition. Physical Review E 70.

Pabst, G., Koschuch, R., Pozo-Navas, B., Rappolt, M., Lohner, K., Laggner, P., 2003. Structural analysis of weakly ordered membrane stacks. Journal of Applied Crystallography 36, 1378-1388.

Parsegian, V.A., 1967. Forces between Lecithin Bimolecular Leaflets Are Due to a Disordered Surface Layer. Science 156, 939-942.

Patel, V.B., Mehta, K., 2015. CHAPTER 1 Betaine in Context, Betaine: Chemistry, Analysis, Function and Effects. The Royal Society of Chemistry, pp. 3-8.

Petrache, H.I., Tristram-Nagle, S., Nagle, J.F., 1998. Fluid phase structure of EPC and DMPC bilayers. Chem.Phys.Lipids 95, 83-94.

Popova, A.V., Busheva, M.R., 2001. Cryoprotective effect of glycine betaine and glycerol is not based on a single mechanism. CryoLetters 22, 293-298.

Rappolt, M., 2010. Bilayer thickness estimations with “poor” diffraction data. Journal of Applied Physics 107, 084701.

Rappolt, M., Hodzic, A., Sartori, B., Ollivon, M., Laggner, P., 2008. Conformational and hydrational properties during the Lβ- to Lα- and Lα- to HII-phase transition in phosphatidylethanolamine. Chemistry and Physics of Lipids 154, 46-55.

Rappolt, M., Laggner, P., Pabst, G., 2004. Structure and elasticity of phospholipid bilayers in the Lα phase: A comparison of phosphatidylcholine and phosphatidylethanolamine membranes, In: Pandalai, S.G. (Ed.), Recent Research Developments in Biophysics. Transworld Research Network, Trivandrum, pp. 365-394.

Rappolt, M., Pabst, G., Amenitsch, H., Laggner, P., 2001. Salt-induced phase separation in the liquid crystalline phase of phosphatidylcholines. Colloids and Surfaces A: Physicochemical and Engineering Aspects 183-185, 171-181.

Rappolt, M., Pressl, K., Pabst, G., Laggner, P., 1998. Lα-phase separation in phosphatidylcholine–water systems induced by alkali chlorides. Biochimica et Biophysica Acta (BBA) - Biomembranes 1372, 389-393.

Rappolt, M., Rapp, G., 1996. Structure of the stable and metastable ripple phase of dipalmitoylphosphatidylcholine. European Biophysics Journal 24, 381-386.

Rudolph, A.S., Crowe, J.H., Crowe, L.M., 1986. Effects of Three Stabilising Agents-Proline, Betaine, and Trehalose-on Membrane Phospholipids. Archives of Biochemistry and Biophysics 245, 134-143.

Rudolph, A.S., Goins, B., 1991. The effect of hydration stress solutes on the phase behavior of hydrated dipalmitoylphosphatidylcholine. Biochimica et Biophysica Acta (BBA) - Biomembranes 1066, 90-94.

Sharma, P., Singh, D.K., Gupta, V., Asthana, B.P., Mishra, P.C., Singh, R.K., 2013. Study of hydration of sarcosine, formation of its zwitterion and their different oligomers in aqueous media: A Raman spectroscopic and theoretical study. Spectroc. Acta Pt. A-Molec. Biomolec. Spectr. 116, 74-83.

Smiatek, J., Harishchandra, R.K., Galla, H.-J., Heuer, A., 2013. Low concentrated hydroxyectoine solutions in presence of DPPC lipid bilayers: A computer simulation study. Biophys. Chem. 180, 102-109.

Söderlund, T., Alakoskela, J.M.I., Pakkanen, A.L., Kinnunen, P.K.J., 2003. Comparison of the effects of surface tension and osmotic pressure on the interfacial hydration of a fluid phospholipid bilayer. Biophysical Journal 85, 2333-2341.

Spaar, A., Salditt, T., 2003. Short Range Order of Hydrocarbon Chains in Fluid Phospholipid Bilayers Studied by X-Ray Diffraction from Highly Oriented Membranes. Biophysical journal 85, 1576-1584.

Sun, W.J., Suter, R.M., Knewtson, M.A., Worthington, C.R., Tristramnagle, S., Zhang, R., Nagle, J.F., 1994. Order and disorder in fully hydrated unoriented bilayers of gel phase dipalmitoylphosphatidylcholine. Physical Review E 49, 4665-4676.

Syamaladevi, R.M., Tang, J., Villa-Rojas, R., Sablani, S., Carter, B., Campbell, G., 2016. Influence of Water Activity on Thermal Resistance of Microorganisms in Low-Moisture Foods: A Review. Comprehensive Reviews in Food Science and Food Safety 15, 353-370.

Takis, P.G., Papavasileiou, K.D., Troganis, A.N., Melissas, V.S., 2015. CHAPTER 4 The Chemistry of Betaine, Betaine: Chemistry, Analysis, Function and Effects. The Royal Society of Chemistry, pp. 47-61.

Tenchov, B., Rappolt, M., Koynova, R., Rapp, G., 1996. New phases induced by sucrose in saturated phosphatidylethanolamines: An expanded lamellar gel phase and a cubic phase. Biochimica et Biophysica Acta - Biomembranes 1285, 109-122.

Thoppil, A.A., Judy, E., Kishore, N., 2017. Mode of action of betaine on some amino acids and globular proteins: Thermodynamic considerations. The Journal of Chemical Thermodynamics 111, 115-128.

Venkatesu, P., Lee, M.-J., Lin, H.-m., 2007. Thermodynamic Characterization of the Osmolyte Effect on Protein Stability and the Effect of GdnHCl on the Protein Denatured State. The Journal of Physical Chemistry B 111, 9045-9056.

Warren, B.E., 1969. X-ray diffraction. Addison-Wesley Pub. Co, Reading.

Wiener, M.C., Suter, R.M., Nagle, J.F., Structure of the fully hydrated gel phase of dipalmitoylphosphatidylcholine. Biophysical journal 55, 315-325.

Wiener, M.C., Suter, R.M., Nagle, J.F., 1989. Structure of the fully hydrated gel phase of dipalmitoylphosphatidylcholine. Biophysical journal 55, 315-325.